Self-guided Laser Wakefield Acceleration Beyond 1 GeV using Ionization-induced Injection

C. E. Clayton, J. E. Ralph, F. Albert, R. A. Fonseca, S. H. Glenzer, C. Joshi, W. Lu, K. A. Marsh, S. F. Martins, W. B. Mori, A. Pak, F. S. Tsung, B. B. Pollock, J. S. Ross, L. O. Silva, D. H. Froula

Disclaimer

This document was prepared as an account of work sponsored by an agency of the United States government. Neither the United States government nor Lawrence Livermore National Security, LLC, nor any of their employees makes any warranty, expressed or implied, or assumes any legal liability or responsibility for the accuracy, completeness, or usefulness of any information, apparatus, product, or process disclosed, or represents that its use would not infringe privately owned rights. Reference herein to any specific commercial product, process, or service by trade name, trademark, manufacturer, or otherwise does not necessarily constitute or imply its endorsement, recommendation, or favoring by the United States government or Lawrence Livermore National Security, LLC. The views and opinions of authors expressed herein do not necessarily state or reflect those of the United States government or Lawrence Livermore National Security, LLC, and shall not be used for advertising or product endorsement purposes.

Self-guided laser wakefield acceleration beyond 1 GeV using ionization-induced injection

C. E. Clayton[1],* J. E. Ralph[2], F. Albert[2], R. A. Fonseca[3,5], S. H. Glenzer[2], C. Joshi[1], W. Lu[1], K. A. Marsh[1], S. F. Martins[3], W. B. Mori[1], A. Pak[1], F. S. Tsung[1], B. B. Pollock[2,4], J. S. Ross[2,4], L. O. Silva[3], and D. H. Froula[2]

[1] *Department of Electrical Engineering, University of California, Los Angeles, CA 90095*
[2] *L-399, Lawrence Livermore National Laboratory, P.O. Box 808, Livermore, CA 94551, USA*
[3] *GoLP/IPFN-LA, Instituto Superior Técnico, Lisboa, Portugal*
[4] *MAE Department, University of California, San Diego, La Jolla, CA 92093 and*
[5] *DCTI/ISCTE - Lisbon University Institute, Lisbon, Portugal*
(Dated: April 19, 2010)

The concepts of matched beam, self-guided laser propagation and ionization-induced injection have been combined to accelerate electrons up to 1.45 GeV energy in a laser-driven, plasma wakefield accelerator. The spatial and spectral content of the laser light exiting the plasma shows that the 60 fs, 110 TW laser pulse is both guided and excites a wake over the entire 1.3 cm length of the gas cell at densities below $1.5 \times 10^{18} \mathrm{cm}^{-3}$. High energy electrons are observed only when small (3%) amounts of CO_2 gas are added to the He gas. Computer simulations confirm that it is the K-shell electrons of oxygen that are ionized and injected into the wake and accelerated to beyond 1 GeV energy.

Recent advances in high-power laser technology have led to major breakthroughs in the field of electron acceleration via the laser wakefield accelerator (LWFA) concept [1]. Among these is the experimental realization of the "bubble" or "blowout" regime [2, 3], where an ultrashort but relativistically-intense laser pulse ($c\tau \lesssim \lambda_p$ and $a_\ell \gtrsim 2$) propagating in an underdense plasma completely blows out all the plasma electrons. Here τ is the full-width at half-maximum laser pulse duration, $a_\ell = \frac{eA}{mc^2}$ is the normalized vector potential of the focused laser pulse and λ_p is the wavelength of the wakefield. These radially-expelled plasma electrons are attracted back towards the laser axis by the space-charge force of the ions, forming a nearly spherical sheath around an "ion bubble" [3]. The electric field created by the resultant charge-density structure—the wakefield—has some distinct advantages: i) an extremely large, radially-uniform accelerating field that propagates at the group velocity of the laser pulse ($\approx c$); ii) a longitudinally uniform but radially-linear focusing field; and iii) the ability to self-guide the laser pulse until it is depleted of its energy [3]. These characteristics are necessary for generating a high-quality, high-energy electron beam in a short distance; i.e., a "tabletop accelerator" [4].

Electrons injected into such an accelerator structure may gain energy until they outrun the wakefield over a dephasing length $L_{dp}[\mathrm{cm}] \simeq (P \ [\mathrm{TW}])^{1/6}(10^{18} \ \mathrm{cm}^{-3}/n_e)^{4/3}$ and gain a maximum energy $W_{max}[GeV] \simeq 0.36(P \ [\mathrm{TW}])^{1/4}(L_{dp}[\mathrm{cm}])^{1/2}$. Here, P is the peak laser power. Therefore, it is in principle possible to accelerate electrons to beyond a GeV energy in a distance of ~ 1 cm using a 100 TW-class laser provided that the electron density n_e is less than $\sim 1.5 \times 10^{18}$ cm^{-3}. The key issues for obtaining W_{max}

are whether the wake can be maintained over L_{dp} and whether electrons can be injected and trapped into the wakefield at such a low density.

The existence of clear spectral features of accelerated electrons in todays LWFA experiments has allowed for systematic studies of the physics controlling the self-guiding [5, 6] of the laser pulse, the electron injection mechanisms [7–10], and the energy of the electron beams. However, the relatively high densities used in these experiments have limited their energy gain to less than 1 GeV. It should be noted that the only previous experiment to report a 1 GeV electron energy gain in a LWFA used a preformed plasma channel to guide the laser pulse [11]. However, using the self-guiding offered by the bubble regime can simplify a practical LWFA.

In this Letter, we show that the concepts of matched-beam, self-guided propagation and ionization-induced injection can be combined, at densities less than 1.5×10^{18} cm^{-3}, to accelerate electrons to beyond 1 GeV in a LWFA. In order to produce the requisite long and uniform volume of low-density gas (beyond the limits of currently-used gas jets [12, 13]), a new target platform was implemented: a 1.3 cm-long cell containing a gas mix of 97% He and 3% CO_2. The spatial and spectral content of the laser light exiting the plasma is measured and is consistent with self-guiding over the entire length of the gas cell ($15 \simeq the vacuum Rayleigh length$) at a plasma density of 1.3×10^{18} cm^{-3}. Full, three-dimensional particle-in-cell (PIC) computer simulations show that it is indeed the K-shell oxygen electrons that are ionized and injected into the wake supported predominantly by the He electrons.

These experiments were performed at the Jupiter Laser Facility, Lawrence Livermore National Laboratory, using
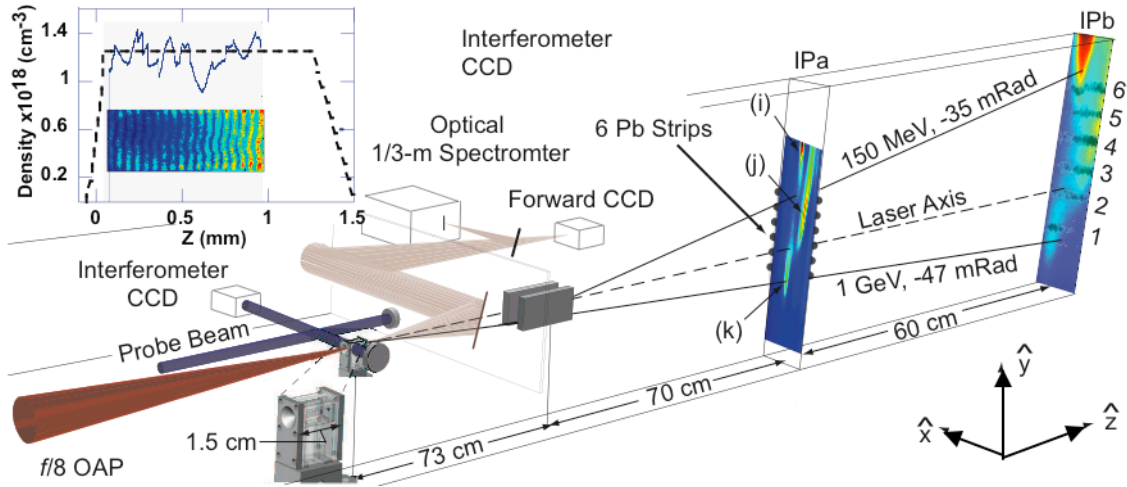
FIG. 1: A schematic of the experiment showing the f/8 laser beam, a blowup of the gas cell, the Michelson interferometer (100 fsec probe duration), the laser exit-spot diagnostics taking reflections from a 5 μm-thick pellicle and an uncoated wedge, the dipole magnet and two successive image plates (IPa and IPb). The image plates show actual experimental results and reveal, in this case, three distinct features in the electron spectrum labeled (i), (j), and (k). Electrons pass through a 40 μm-thick aluminum optical dump and a 63 μm-thick Mylar vacuum window (neither shown). Also shown are two electron trajectories and dimensions. Inset: Interferogram, the abel-inverted, on-axis density (solid line) and estimated complete n_e profile (dashed line). The up-ramp at the cell entrance is about 0.5 mm and down-ramp at the cell exit is estimated to occur over 2 mm; the size of the entrance and exit apertures on the gas cell, respectively. The laser is polarized along $\hat{x}$.

the 250 TW, 60 fsec Ti:Sapphire Callisto Laser System. Figure 1 shows the experimental setup where the laser beam was focused onto the front of the gas cell. The vacuum spot size w_0 was measured at low powers to be 15 μm at the $1/e^2$ intensity point. The fractional laser energy contained within the central laser spot was measured to be $\sim 50\%$ which will be taken into account when quoting peak power in the remainder of this paper. The plasma density is measured using interferometry to be $1.3 \pm 0.1 \times 10^{18}$ cm^{-3} over the first 0.8 cm and inferred to have a 1.3 cm long plateau, as shown in the inset to Fig. 1.

The electron beams produced by this laser wakefield accelerator were characterized using a two-screen spectrometer as shown in Fig. 1. This system provides an accurate measurement of the energy of the electrons, the vertical (horizontal) angle θ_{0y} (θ_{0x}) that the electrons exit the plasma relative to the original laser axis, the x-divergence, and the electron charge [14–16]. The electrons exiting the plasma are deflected in the $+\hat{y}$-direction by a 20-cm long, 0.46 Tesla dipole magnetic field. The electrons are detected by two successive image plates allowing for a unique solution to their energy and θ_{0y} provided common spatial features can be identified on both image plates. When a broad spectrum is generated, spatial features must be imposed on the second image plate (IPb) and this is accomplished by the six lead fiducials just behind the first image plate (IPa), as shown in Fig. 1. From the "shadows" cast by the Pb strips onto IPb, labeled 1–6 in Fig. 1, six independent measurements of the electron energies and θ_{0y}'s are obtained. The image

plates are calibrated to directly provide electron charge [17].

Figure 2(a) shows that the measured $1/e^2$ laser spot at the exit of the plasma is about 24 μm. This is ≈ 15 times smaller than it would be for vacuum propagation and suggests that the laser beam is guided over the entire 1.3 cm length of the plasma (to within the 1 mm depth-of-focus of the imaging system). Indeed, PIC simulations and associated phenomenological theory [3] show self-guiding occurs at a "matched" spot size $w_m \simeq 2\sqrt{a_\ell}/k_p$; the blow-out process near the front of the pulse creates a refractive-index channel which balances diffraction. This regime is accessed provided that $a_\ell \gtrsim 2$ and $w_0 \approx w_m$. For the conditions in this experiment, P = 110 TW and
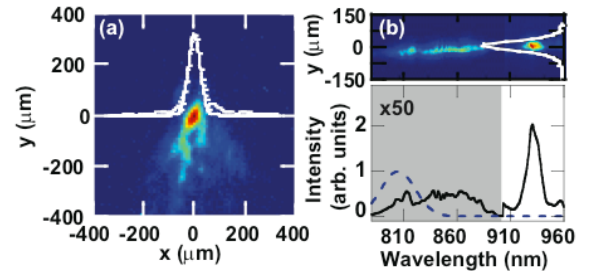

FIG. 2: (color)(a) The laser spot at the exit of the gas cell. (b) Spectrally– and spatially–resolved (in $\hat{y}$) laser spot at the exit of the gas cell. Note that the spectrum up to 900 nm has been suppressed by 50$\times$ to compensate for the falling quantum efficiency of the CCD camera at longer wavelengths. The original laser spectrum (dashed line) is also shown.
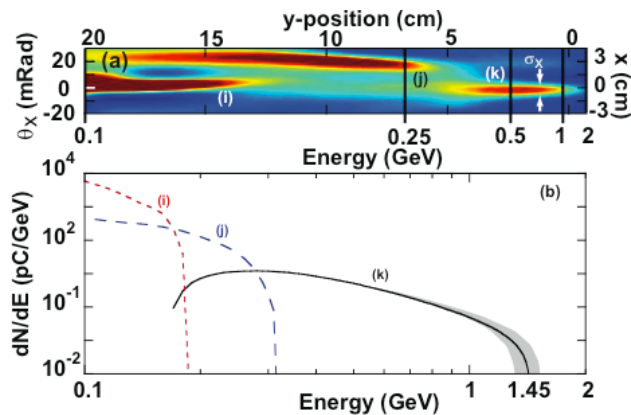
FIG. 3: (a) Raw electron data from IPa with θ_x and energy scales. Three clear features are labeled (i), (j) and (k). Location of line-out for $D_x(\theta)$ for finding σ_x (white arrows, see text). (b) Electron spectra for the three features of (a). Uncertainty in θ_{0y} indicated by shaded region for curve (k) (negligible for curves (i) and (j)).

$n_e = 1.3 \times 10^{18}$ cm^{-3}, $w_m \simeq 17$ μm which is close to w_0 of 15 μm. This self-guided laser pulse will excite the wake over the entire length of the gas cell because the nonlinear pump-depletion length $L_{pd} \approx \frac{\omega_0^2}{\omega_p^2} c\tau$ is about 2.1 cm. This is longer than the gas cell length which was chosen to be close to L_{dp}.

Furthermore, Fig. 2(b) shows that the light within the guided spot has been significantly red shifted indicating that a nonlinear wake has been driven to the end of the plasma [5]. At this plasma density, $c\tau \approx \lambda_{p,NL}/2$ where $\lambda_{p,NL} \simeq 2w_m$ is the nonlinear wavelength of the wake. Thus this experiment is in the ideal wakefield regime; i.e., nearly all the laser photons reside in the first half-wavelength of the wake. Therefore the photons are expected to be both red-shifted [3] and guided by the wake which is evident in the spatially-confined but strongly red-shifted spectrum shown in Fig. 2(b).

Although it is clear from Fig. 2 that it is possible to excite a wake over the entire length of the gas cell, electrons were never observed in similar experiments using pure He plasmas for laser powers of up to 120 TW at $n_e \lesssim 3 \times 10^{18}$ cm^{-3} [12, 13, 18, 19]. The spectrum shown in Fig. 3 was obtained on a 110 TW laser shot at $n_e \simeq 1.3 \times 10^{18}$ cm^{-3} after adding 3% CO_2 to the gas cell. At this low density and for $a_\ell \lesssim 4$, only electrons born *inside* the ion bubble are expected to be trapped via "ionization-induced injection" [7] (see later).

We first discuss the highest-energy feature (k) of the three spectral features apparent in Figure 3(a). This feature is spatially narrow indicative of a beam of high-energy electrons, and (on the face of it) extends to an energy of about 2 GeV when only accounting for the magnet dispersion for a beam exit angle θ_{0y}. However, after correcting for the angular spread of the electrons around

θ_{0y}, the maximum energy is found to be 1.45 ± 0.1 GeV, as seen in spectrum (k) of Fig. 3(b). The procedure that leads to this spectrum is as follows: lead strips 1 and 2 indicate a $\theta_{0y} = -47 \pm 2$ mrad at the respective energies of 415 MeV and 278 MeV. This exit angle is used to generate the spectrum (dN/dE vs. electron energy E above 200 MeV) shown in Fig. 3(b) after deconvolving the estimated spread in y-angles $D_y(\theta)$ of the electron beam at IPa. To first order, we assume that $D_y(\theta)$ is the same as the corresponding x-angular spread $D_x(\theta)$ and thus take $D_y(\theta)$ as a Gaussian fit to an x-lineout of the data at $y = 2$ cm (top scale of Fig. 3(a)). The deconvolution is $dN/dE = dN/dy \times \sum_\theta (D_y(\theta) \times dy(\theta)/dE)$ where dN is the number of electrons in a bin, dN/dy is the raw IPa data, dy/dE is the calculated dispersion at IPa for all values of θ, and $D_y(\theta)$ has been centered on θ_{0y} and has an RMS spread $\sigma_\theta \simeq 4.4$ mrad as indicated in Fig. 3(a). The uncertainty of ± 2 mrad in the central value of θ_{0y} gives rise to the uncertainty in spectrum (k), represented by the shaded area in Fig. 3(b). We see that there is clearly signal up to 1.45 ± 0.1 GeV. The total charge in this feature is about 3.8 pC. Taking the dephasing-length-averaged accelerating field $E_z \approx 0.5\sqrt{a_\ell}mc\omega_p/e \simeq 1.1$ GeV/cm [3] gives a W_{max} of about 1.4 GeV for an acceleration length of 1.3 cm, consistent with the experiment.

Since the two-screen spectrometer allows for the simultaneous determination of θ_{0x} and θ_{0y}, such data can be used to provide insight into the origins of the two lower-energy electron features labeled (j) and (i) in Fig. 3. We first note that features (j) and (i) are much lower in energy than feature (k). Regarding feature (j), $\theta_{0x,j} - \theta_{0x,k} \approx 22$ mrad, a difference which is much greater than σ_θ. This large difference in both the energy of the electrons and their x-angle of exit from the plasma suggests that the electrons forming feature (j) are from a different accelerating bucket. Similarly, for feature (i), $\theta_{0y,i} - \theta_{0y,k} \simeq -21$ mrad, again larger than σ_θ. This large difference in the exiting y-angle and energy between features (i) and (k) suggest that the electrons forming feature (i) are from yet another accelerating bucket of the wake. Since there are no self-trapped electrons without CO_2 and all the trapped electrons presumably originate in the first bucket, a "leaky" first bucket may be responsible for populating subsequent buckets.

Three-dimensional PIC simulations of the experiment have been carried out using the code OSIRIS which employs a speed-of-light window and tunnel-ionization of a multi-species gas [20]. The simulation used a 93 by 112 by 112 μm computational box corresponding to 3200 by 128 by 128 grid points with a resolution along the laser propagation direction of 290 nm and 870 nm in the transverseness plane. Four species were used: He, C, L-shell O, and K-shell O, corresponding to about 5.2e8 total particles in the simulation box. Figure 4(a) shows that at a distance of 1.75 mm into the gas, much of the laser pulse resides in the fully blown-out ion bubble. The elec-
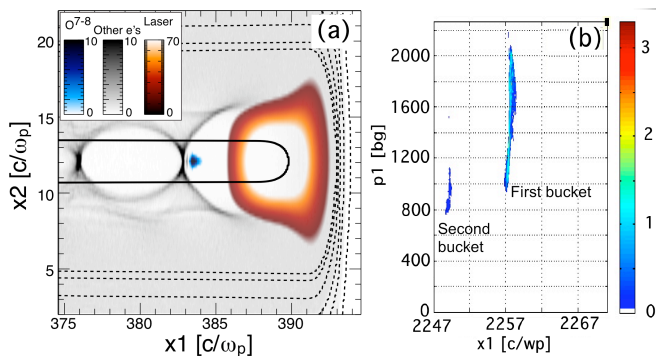
FIG. 4: Results from a 3D PIC simulation for experimental parameters. (a) Contour maps of: the envelope of the laser field (orange-white, right colorbar, statvolts/cm); the electron-density contribution from He, C, and the L-shell electrons of O (grey, center colorbar, n/n_e); and the electron-density contribution from the K-shell of O (blue, left colorbar, n/n_e) at a distance of 1.75 mm into the simulation. The longitudinal position where the L-shell (K-shell) O electrons were ionized; dashed lines (solid line). (b) Spectrum of K-shell O electrons from simulation in charge per bin (AU).

trons from helium, carbon, and the L-shell of oxygen are ionized by the very front of the laser pulse and are immediately blown out, forming a sheath around the ion bubble. The figure also shows the ionization contour of the K-shell oxygen electrons. For laser intensities of 1.6 (2.4) $\times 10^{19}$ W/cm^2 or $a_\ell > 2.7$ (3.3), we expect O^{+7} (O^{+8}) to be produced. Given that our peak intensity at 110 TW is about 3×10^{19} W/cm^2, the K-shell electrons are born near the peak of the laser (within the bubble), thus allowing for their trapping [7]. As the laser propagates through the first 2.5 mm of the plasma, K-shell electrons of O are continuously injected. Beyond this point in the simulation, however, the peak laser intensity falls below the tunnel-ionization threshold to produce O^{+7}. However the intensity remains high enough to both guide the laser pulse and excite the wake over an ≈ 1 cm propagation distance. Some of these K-shell electrons (blue cluster at the back of the first bucket) are trapped by the wake and gain energy. An insignificant number of C K-shell electrons have been trapped in the first bucket. Figure 4(b) shows the longitudinal phase space of the O K-shell electrons after propagating 1 cm through the plasma. The high energy electrons reside in the first bucket and have a continuous spectrum extending out to 1.1 GeV. Some of the electrons that were born in the first bucket leak out and are trapped in the second bucket. Both the spectrum and multiple buckets seen in the simulation are in qualitative agreement with the experiment. The lowest-energy feature in the experiment (~ 100 MeV) could be cut off by the length of the simulation box.

It is clear from this simulation that no electrons above 400 MeV can be observed at this low density without ionization-induced injection of O^{+7} and O^{+8} electrons

into the wake. The energy spectrum of these electrons could be made narrower by optimizing the beam loading (by controlling the oxygen concentration and the laser intensity profile), thereby limiting the distance over which the electrons are injected into the wake.

In conclusion, we have shown that an ultrashort laser pulse can be self-guided by the wake over a distance of greater than one centimeter in a low density plasma. Electrons can be injected into such a wake using ionization-induced injection and be accelerated up to 1.45 GeV, close to the dephasing-limited maximum energy gain.

References

* Electronic address: cclayton@ucla.edu
[1] T. Tajima and J. M. Dawson, Phys. Rev. Lett. **43**, 267 (1979).
[2] A. Pukhov and J. Meyer-ter Vehn, Appl. Phys. B **74**, 355 (2002).
[3] W. Lu et al., Phys. Rev. ST Accel. Beams **10**, 061301 (2007).
[4] C. Joshi, Sci. Am. **294**, 40 (2006).
[5] J. Ralph et al., Phys. Rev. Lett. **102**, 175003 (2009).
[6] A. G. R. Thomas et al., Phys. Rev. Lett. **98**, 095004 (2007).
[7] A. Pak et al., Phys. Rev. Lett. **104**, 025003 (2010).
[8] C. McGuffey et al., Phys. Rev. Lett. **104**, 025004 (2010).
[9] J. Faure et al., Nature **444**, 737 (2006).
[10] S. P. D. Mangles et al., Phys. Rev. Lett. **96**, 215001 (2006).
[11] W. P. Leemans et al., Nat. Phys. **2**, 696 (2006).
[12] S. Kneip et al., Phys. Rev. Lett. **103**, 035002 (2009).
[13] N. A. M. Hafz et al., Nat Photon **2**, 571 (2008).
[14] I. Blumenfeld et al., Nature **445**, 741 (2007).
[15] B. B. Pollock et al., in *Proceedings of the 2009 Particle Accelerator Conference* (Vancouver, Canada, 2009).
[16] C. E. Clayton et al., J. Instrum. (to be submitted).
[17] N. Nakanii et al., Rev. Sci. Instrum. **79**, 066102 (2008).
[18] D. H. Froula et al., Phys. Rev. Lett. **103**, 215006 (2009).
[19] J. E. Ralph et al., Phys. Plasma *to be published* (2010).
[20] R. A. Fonseca et al. (Heidelberg: Springer, 2002), vol. 2331 of *Lecture Notes on Computer Science*, pp. 342–351.